Journal of Great Lakes Research 42 (2016) 536–548

Contents lists available at ScienceDirect

Journal of Great Lakes Research

journal homepage: www.elsevier.com/locate/jglr

Simulated impacts of climate change on phosphorus loading to Lake Michigan

Dale M. Robertson [a,*], David A. Saad [a], Daniel E. Christiansen [b], David J. Lorenz [c]

[a] U.S. Geological Survey, Wisconsin Water Science Center, 8505 Research Way, Middleton, WI 53562, USA
[b] U.S. Geological Survey, Iowa Water Science Center, 400 S. Clinton St., Iowa City, IA 52240, USA
[c] University of Wisconsin, Center for Climatic Research, 1225 West Dayton St., Madison, WI 53706, USA

ARTICLE INFO

Article history:
Received 25 January 2016
Accepted 26 February 2016

Communicated by Craig Stow

Index words:
Phosphorus
Loading
Streamflow
Climate change

ABSTRACT

Phosphorus (P) loading to the Great Lakes has caused various types of eutrophication problems. Future climatic changes may modify this loading because climatic models project changes in future meteorological conditions, especially for the key hydrologic driver — precipitation. Therefore, the goal of this study is to project how P loading may change from the range of projected climatic changes. To project the future response in P loading, the HydroSPARROW approach was developed that links results from two spatially explicit models, the SPAtially Referenced Regression on Watershed attributes (SPARROW) transport and fate watershed model and the water-quantity Precipitation Runoff Modeling System (PRMS). PRMS was used to project changes in streamflow throughout the Lake Michigan Basin using downscaled meteorological data from eight General Circulation Models (GCMs) subjected to three greenhouse gas emission scenarios. Downscaled GCMs project a +2.1 to +4.0 °C change in average-annual air temperature (+2.6 °C average) and a −5.1% to +16.7% change in total annual precipitation (+5.1% average) for this geographic area by the middle of this century (2045–2065) and larger changes by the end of the century. The climatic changes by mid-century are projected to result in a −21.2% to +8.9% change in total annual streamflow (−1.8% average) and a −29.6% to +17.2% change in total annual P loading (−3.1% average). Although the average projected changes in streamflow and P loading are relatively small for the entire basin, considerable variability exists spatially and among GCMs because of their variability in projected future precipitation.

Introduction

The Laurentian Great Lakes constitute the largest freshwater system in the world, and have about 10% of the United States (U.S.) and 30% of the Canadian populations in their watersheds. The Great Lakes receive water and accompanying nutrients from many tributaries draining areas ranging from pristine forests, to intensively farmed areas, to large urban centers, and nutrient input from these tributaries is extremely variable (Rathke and McRae, 1989; Robertson, 1997; Robertson and Saad, 2011). This nutrient loading has caused eutrophication to various degrees and scales, from selected bays around the Great Lakes (e.g., Green Bay in Lake Michigan) to wide-scale eutrophication in some of the Great Lakes themselves (e.g., Lake Erie; Michalak et al., 2013). The Great Lakes Water Quality Agreement (GLWQA, signed in 1972) identified phosphorus (P) as the nutrient of primary concern for eutrophication of the Great Lakes and defined target P loads for each lake. Since the implementation of the GLWQA, P loading to each Great Lake (except Lake Superior) has been reduced (Dolan and Chapra, 2012), which has reduced most open-lake eutrophication problems, except for Lake Erie (Zhou et al., 2013); however, eutrophication problems are still common in many nearshore areas (Schultze, 2005), embayments (DePinto et al., 2006), and even much of Lake Erie (Michalak et al., 2013). Because of continuing eutrophication problems, the original P loading targets are now being revised (USEPA, 2015). To develop plans to obtain P loading below these targets and develop reduction strategies to decrease the eutrophication problems, it is important to understand how future climatic changes in the Great Lakes Basin (GLB) may affect P loading and how these changes compare with those that have been projected with changes in land use.

Nutrient (P) loading in a stream is a function of its water quality (P concentrations) and streamflow. Any changes in the factors affecting the concentrations or streamflow may change the P loading in a stream. Water quality in streams has been shown to be strongly related to land use (for example, see SWAT [Soil and Water Assessment Tool; Arnold et al., 2012] and SPARROW [Spatially Referenced Regression On Watershed attributes model; Robertson and Saad, 2011] modeling applications), and streamflow has been shown to be strongly related to precipitation, and to a lesser degree air temperature (for example, see

* Corresponding author. Tel.: +1 608 821 3867.
E-mail addresses: dzrobert@usgs.gov (D.M. Robertson), dasaad@usgs.gov (D.A. Saad), dechrist@usgs.gov (D.E. Christiansen), dlorenz@wisc.edu (D.J. Lorenz).

http://dx.doi.org/10.1016/j.jglr.2016.03.009
0380-1330/

PRMS [the Precipitation-Runoff Modeling System hydrologic watershed model; Markstrom et al., 2015]). Therefore, in the future, P loading from the GLB may change as a result of future changes in land use and climate. Here, we summarize how projected changes in climate alone have been projected to affect streamflow in all of the tributaries to one of the Great Lakes (Lake Michigan) (described in detail by Christiansen et al., 2014), and then couple these results with concentration and in-stream-decay information from the landscape-scale SPARROW fate and transport watershed model (Robertson and Saad, 2011) to project future changes in P loading from the Lake Michigan Basin (LMB). We then compare these results with what has been projected to be transported from the LMB as a result of specific future land-use scenarios in the absence of climatic change (LaBeau et al., 2014).

Land use in the GLB has changed rather dramatically over recent decades (Nechyba and Walsh, 2004) and is expected to continue to change in the future. To estimate the effects of future changes in land use on P delivery from the GLB from 2010 to 2040, LaBeau et al. (2014) coupled the landscape-scale SPARROW P model (Robertson and Saad, 2011) with projections from the Land Transformation Model (LTM) (Pijanowski et al., 2002). According to LTM predictions for specific urban expansion and agricultural scenarios, the GLB may experience a doubling of urbanized areas and a 10% increase in agricultural areas through biofuel feedstock cultivation. These land-use changes by 2040 were projected to increase P loadings from the U.S. side of the GLB by 3.5–9.5%, depending on the lake basin and development scenario. The exception was Lake Ontario, where loading was projected to decrease by 1.8% for one scenario, due to population losses in its U.S. drainage area. Overall by 2040, urban expansion in the LMB was estimated to increase P loadings by 4.9%, and additional agricultural expansion associated with predicted biofuel feedstock cultivation was estimated to further increase P loadings by 4.8%, for a total increase in P loading to Lake Michigan (LM) by 9.8%.

The climate of the GLB is also projected to change. The two primary driving forces of climate change that affect hydrology and ultimately the P loading are air temperature and precipitation. In general, results from General Circulation Models (GCMs) project that air temperatures in the GLB will increase 2–5 °C by the middle of this century, with largest changes in winter, and spatial and temporal precipitation patterns may change, with most GCMs predicting increases in precipitation in fall, winter, and spring, and decreases during summer (WICCI, 2011). The forecasted changes in precipitation are less certain than those for temperature, but most models predict annual precipitation will increase (WICCI, 2011).

GCMs predict large-scale changes (grid units typically cover 100s km^2) in air temperature and precipitation, but they are limited in describing changes at smaller scales, such as the basins of selected tributaries to the Great Lakes. Therefore, daily downscaled climate projections, for nine GCMs that each simulated the effects of three different greenhouse gas emission scenarios, were developed for Eastern U.S. (Notaro et al., 2011, 2014). Only eight of these GCMs had complete results for the three different greenhouse gas emission scenarios used in this study, and therefore were used here. For each GCM, baseline current downscaled conditions throughout this area were first simulated and evaluated, and then future downscaled conditions were estimated for each of the various greenhouse gas emission scenarios during the 21st century.

To determine how these future changes in air temperature and precipitation may affect streamflow in the LMB, Christiansen et al. (2014) developed a coarse-scale PRMS model for the entire LMB for present conditions, and then input the downscaled daily air temperatures and precipitation from eight GCMs developed by Notaro et al. (2011, 2014) to project streamflow in the middle and late part of the 21st century. They found that, on average, future climate change may cause a slight decrease in annual streamflow, but results varied by GCM and season.

The goals of this paper are to: 1) describe the HydroSPARROW approach—that can be used to project future changes in nutrient loading from large watersheds associated with climate or land-use change; 2) describe the projected changes in P loading to LM caused by projected changes in climate and hydrology; 3) compare our results with those of other studies conducted on tributaries to the Great Lakes examining the effects of climate change, and 4) compare the relative importance of climate change and land-use change on future P loading to LM, by comparing our results induced by climate change with those projected by LaBeau et al. (2014) for land-use change. To do this, we first briefly describe the downscaled changes in air temperature and precipitation (Notaro et al., 2011, 2014) and streamflow (Christiansen et al., 2014) projected for the LMB, and then use this information with HydroSPARROW to project changes in P loading that may occur during the 21st century.

Methods

HydroSPARROW

To project how future climate change may affect P loading into LM, the HydroSPARROW approach was developed that links results of two spatially explicit models, the transport and fate watershed model SPARROW and the water-quantity model PRMS (Fig. 1). To simulate the effects of changes in climate with HydroSPARROW, P loading from each SPARROW catchment is first divided into the two components making up the long-term (~30 years) average-annual detrended loads: average-annual flow and the corresponding volumetrically weighted P concentration. Each of these two components for each catchment is then adjusted to represent future conditions. Flows are modified using PRMS results, and volumetrically weighted P concentrations are modified to incorporate the effects on in-stream/in-reservoir decay caused by changes in travel time (described below). Finally, the future P concentrations are multiplied by the future average-annual flows to obtain future P loading from each catchment. This approach has also been used to simulate the effects of future changes in land use by using SPARROW to estimate future changes in P concentrations (LaBeau et al., 2014). In that application of HydroSPARROW, streamflow was assumed to remain unchanged. Results for each catchment are then evaluated for spatial patterns and aggregated to estimate the total input over large areas.

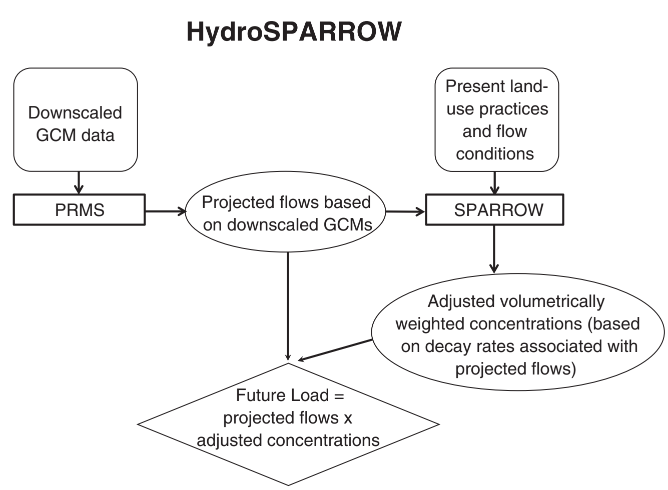

Fig. 1. Schematic demonstrating the HydroSPARROW approach, which uses inputs from General Circulation Models (GCMs), and outputs from the Precipitation Runoff Modeling System (PRMS) and the SPAtially Referenced Regression on Watershed attributes (SPARROW) model.

SPARROW

SPARROW is a GIS-based watershed model that uses a mass-balance approach to estimate the non-conservative transport and transformation (i.e., losses) of nutrients under long-term steady-state conditions in relation to statistically significant landscape properties, such as climate, soils, and artificial drainage (Schwarz et al., 2006). SPARROW is a spatially explicit model that estimates nutrient loading from a series of hydrologically linked catchments. SPARROW models simulate long-term mean-annual nutrient transport given nutrient inputs similar to a given base year (for use in this study, it was calibrated for inputs similar to 2002). For the calibrated SPARROW model for the Upper Midwest (Robertson and Saad, 2011), P sources included point sources (from wastewater treatment plants and industrial sources), manure, farm fertilizers, and forested and urban lands. Statistically significant land-to-water delivery variables, also referred to as spatial variability factors, are incorporated into the model to describe the variability in the amount of nutrients from each source transported to the stream network. For this P model, this included soil permeability and the percentage of the catchment having tile drains. Part of the nutrient flux reaching the streams is then attenuated or decayed during downstream transport. SPARROW models typically have variables that describe losses in the stream network, which are estimated as a function of travel time in streams and areal hydraulic load in reservoirs (Schwarz et al., 2006), both of which should change with changes in streamflow and therefore need to be adjusted when using HydroSPARROW (described below). A brief overview of the SPARROW model is provided in the Electronic Supplementary Material (ESM) Appendix S1, and a detailed description of the model is given in Schwarz et al. (2006).

To obtain the initial information needed for HydroSPARROW, P loading from each SPARROW catchment in the LMB was divided into long-term average-annual flow (Brakebill and Terziotti, 2011) and corresponding volumetrically weighted P concentrations (SPARROW estimated loads divided by average-annual flow). Volumetrically weighted P concentrations may change with changes in streamflow because of changes in in-stream and in-reservoir decay; therefore, first we need to project how streamflow throughout the LMB will change in response to the projected changes in climate (air temperature and precipitation).

Table 1
General Circulation Model (GCM) outputs used in this study from the World Climate Research Programme's Coupled Model Intercomparison Project phase 3 (CMIP3) multimodel dataset archive.

GCM abbreviation	GCM	Description
CGM3	CGCM-3.1	Canadian Centre for Climate Modeling and Analysis, Canada
CNRM	CNRM-CM-3	Meteo-France/Centre National de Recherches Meteorologiques, France
CSIRO	CSIRO-MK-3.5	Commonwealth Scientific and Industrial Research Organisation (CSIRO) Atmospheric Research, Australia
GFDL	GFDL-CM-2.0	U.S. Department of Commerce, National Oceanographic and Atmospheric Administration, Geophysical Fluid Dynamics Laboratory (GFDL), USA
GISS	GISS-ER	U.S. National Aeronautics and Space Administration, Goddard Institute for Space Studies (GISS), USA
MIUB	ECHO-G	Meteorological Institute of the University of Bonn, Meteorological Research Institute of the Korea Meteorological Administration (KMA), and Model and Data Group, Germany/Korea
MPI	ECHAM5/MPI-OM	Max Planck Institute for Meteorology, Germany
MRI	MRI-CGCM-2.3.2	Meteorological Research Institute, Japan

Downscaled meteorological conditions

To project how air temperature and precipitation in the LMB may change in the future, results from eight large-scale GCMs (Table 1) from the Climate Model Intercomparison Project Phase 3 (CMIP3) were downscaled on a daily basis for the eastern U.S. (Notaro et al., 2011, 2014). Each GCM simulated the effects of four different greenhouse gas emission scenarios (present conditions: 1981–2000, and three future scenarios for the entire 21st century). The three future scenarios represent the low-end (scenario—B1; population peaking in the middle of the 21st century and then declining, with reductions in material intensity and the introduction of clean and resource efficient technologies), most likely (scenario—A1B; population peaking in the middle of the 21st century and then declining, with the rapid introduction of new and more efficient technologies balanced on all energy sources), and high-end (scenario—A2; continuing population growth with highest emissions) in terms of projected greenhouse gas emissions (IPCC, 2007; Nakicenovic et al., 2000).

Downscaling of daily minimum and maximum temperature and precipitation was conducted at $0.1° \times 0.1°$ resolution (Notaro et al., 2011, 2014). Downscaling was done in a probabilistic manner because a specific large-scale state does not determine a single precise value of temperature or precipitation at a specific location, but rather the parameter values in a parametric probability density function (PDF). To create a gridded downscaling dataset, the PDF parameters were interpolated to a predefined grid by using weather data from approximately 4000 stations in the National Weather Service (NWS) Cooperative Observer Program (1950–2009) and the Environment Canada database (1950–2007) to train the statistical models. To generate "normal" data from the PDF parameters, random numbers were drawn from the PDFs, generating a possible realization of the small-scale state that was consistent with the large-scale fields. The random numbers were correlated in space (and time, in the case of temperature) so that the spatial and temporal correlations of the downscaled variables were similar to observations. The downscaling performed well in reproducing both the mean and the variability in precipitation and temperature, including the extremes (Vavrus et al., 2015). The extremes were well simulated because the PDF approach characterizes the portion of the variability not "explained" by the large-scale. This approach was used to develop downscaled daily air temperatures and precipitation for the three periods (1981–2000, 2046–2065, and 2081–2100).

Recently, GCM results have been updated as part of CMIP5 (Taylor et al., 2012). Overall, the multi-model ensemble mean performance did not improve substantially in CMIP5 relative to CMIP3 for precipitation, but there was a slight improvement for near-surface air temperature over land (Sheffield et al., 2014). However, the original biases in air temperature in CMIP3 were already dramatically reduced as part of the downscaling process. The new projections have a slightly larger overall spread in predicted changes in air temperature and precipitation than those used in this study from CMIP3, primarily because additional GCMs were examined and because a wider range in greenhouse gas emission scenarios were examined (Sheffield et al., 2014; Sun et al., 2015). In addition, there appears to be a slightly higher probability that precipitation may increase in the Midwest part of the U.S. (Sun et al., 2015). Therefore, the plausible range in climatic variables, and resulting streamflow and P loading may be slightly larger if CMIP5 results were used in this analysis. Results from CMIP5 have not yet been downscaled using the approach developed by Notaro et al. (2011, 2014).

Streamflow

To project future streamflow throughout the LMB, a PRMS model was constructed for the entire LMB (Christiansen et al., 2014). PRMS is a modular, deterministic, distributed parameter, physically based model developed to simulate basin conditions and surface-water runoff resulting from the effects of meteorological forcing and land cover using physical laws and empirical relations (Markstrom et al., 2015). Modeled basins are first divided into a series of piecewise-constant contiguous spatial units, called hydrologic response units (HRUs), based on hydrologic and physical characteristics such as land-surface altitude, slope, aspect, plant type and cover, land use, soil morphology, geology, drainage boundaries, distribution of precipitation, air temperature, solar radiation, and flow direction. An energy balance and a water balance are then computed for each HRU on a daily time step. PRMS uses minimum and maximum daily air temperatures, and precipitation as primary meteorological drivers (snowfall was estimated from precipitation when air temperatures were below freezing) and calibrated using solar radiation, potential evaporation, and streamflow measured throughout the basin being modeled. For calibration of the LMB PRMS model, weather datasets were collected from 157 stations with data that covered the majority of the time period from 1969 to 2008. To evaluate the accuracy of the LMB PRMS model, Nash–Sutcliffe efficiency (NSE) values (Moriasi et al., 2007) were computed for monthly mean streamflows and monthly mean baseflows. The NSE values were above 0.50 (greater than 0.50 is satisfactory) for 85% of the calibration locations for monthly mean observations and 60% of the calibration locations for monthly mean baseflow observations. After the LMB PRMS was calibrated with historical measured data, the downscaled GCM outputs for daily minimum and maximum temperature and precipitation for three periods (1981–2000, 2046–2065, and 2081–2100) were entered as new input to the model. The LMB PRMS model was then used to predict daily streamflows based on the results from the eight downscaled GCMs described in Table 1, each model applied to present conditions and the three future greenhouse gas emission scenarios. The 20 years for each period include wet and dry years, and the effects of potential changes in precipitation intensity on streamflow. The daily streamflows were then summarized into long-term average-annual streamflow for each of the three periods for each SPARROW catchment.

Volumetrically weighted phosphorus concentrations

The average-annual volumetrically weighted P concentrations from the original SPARROW model were adjusted to reflect changes in in-stream and in-reservoir losses based on the simulated future flows for each scenario and their corresponding estimated water velocities and travel times. Future velocities in each stream reach were calculated as a function of the projected long-term average streamflows for each period and stream order, similar to the original SPARROW model (see Schwarz et al., 2006; Alexander et al., 1999). Future in-stream and in-reservoir losses were then simulated in SPARROW as a function of the new travel time through the stream reach (water velocity divided by stream reach length) for streams and for reservoirs as a function of their surface area divided by the annual streamflow discharging from the reservoir. Future volumetrically weighted P concentration for each catchment for each scenario and period was computed using interim loads computed with the SPARROW model using in-stream and in-reservoir loss rates based on projected future streamflows and velocities and the average-annual flows from the original model (Brakebill and Terziotti, 2011). This provided future P concentrations adjusted only for the estimated changes in in-stream and in-reservoir loss rates.

Finally, the future long-term average volumetrically weighted P concentrations for each SPARROW catchment are multiplied by the corresponding future long-term average-annual flows estimated from PRMS for each period for each GCM and scenario to obtain future P loading (Fig. 1). Future P loadings from all SPARROW catchments were then evaluated for spatial patterns and aggregated to estimate the total input from the entire LMB for each scenario.

Results

Simulated results (by GCM and emission scenario, and selected averages) of air temperature, precipitation, streamflow, P loading, and volumetrically weighted P concentrations for the entire LMB are summarized for the present (1981–2000) and middle of the 21st century (2046–2065) in Table 2, and for the end of the 21st century (2081–2100) in ESM Table S2.

Present (1981–2000) base conditions

Simulated average-annual air temperatures for the 1981–2000 base period (average of the eight GCMs) ranged from 2.7 °C in the northwest part of the LMB to 11.3 °C in the southern part (Notaro et al., 2011, 2014) (Fig. 2a). Simulated average total annual precipitation ranged from 750 mm in the northwest part of the LMB to 1010 mm in the southeastern part (Fig. 2b). There is a northwest to southeast gradient in air temperatures and precipitation caused by the effects of the Great Lakes, with warmer and wetter conditions on the southeast side of LM.

Simulated average-annual streamflow for the base period ranged from <1 m^3/s in small headwater areas to 174 m^3/s in the mouths of the major tributaries (Fig. 2c). Highest unit-area contributions to flow (yields) come from the northern and eastern sides of the LMB (Fig. 2d). The total simulated average-annual streamflow to LM for 1981–2000 was 11% higher than that used in the original SPARROW model (1365 m^3/s, Table 2, compared to 1232 m^3/s used in SPARROW: estimated for 1975–2007 from Brakebill and Terziotti, 2011).

Long-term average P loading for the early 2000s (direct output from the original Robertson and Saad [2011] SPARROW model) ranged from <1 kg/year in small headwater areas to 668,000 kg/year at the mouth of the Grand River (Fig. 3a). Because loads are directly related to flow, the loads generally increase with increasing stream size. To use HydroSPARROW, the total P load in each SPARROW catchment was converted into the components making up the loads: annual-average flow (similar to the streamflows in Fig. 2c) and the corresponding volumetrically weighted P concentrations (Fig. 3b). The volumetrically weighted P concentrations have a north-to-south gradient driven by the distribution in land use, with highest concentrations in areas dominated by agriculture and urbanization. Volumetrically weighted P concentrations are especially high in the intense agricultural areas on the west shore of LM.

The pattern in simulated average-annual total P loading throughout the LMB from HydroSPARROW (average of that for the eight GCMs) for 1981–2000 was very similar to those in Fig. 3a. The total simulated average-annual P loading to LM from HydroSPARROW for this period was 4640 MT (Table 2), which is 14% higher than that estimated in the original SPARROW model (4061 MT) because the average-annual streamflows estimated with PRMS were 11% higher than those used in the original SPARROW model. This estimate of total loading to LM is also higher than that estimated by Dolan and Chapra (2012) for 1994–2008 (3175 MT; values in their Table 6 with contributions from atmospheric deposition removed). Although the loads estimated with HydroSPARROW may be slightly different than these other estimated loads, the relative differences in P loading to LM projected with HydroSPARROW should be suitable for evaluating the effects of climate change. HydroSPARROW load estimates should be relatively insensitive to compounding errors and additional biases because the model errors in both PRMS and SPARROW should equally affect both the estimates of the baseline and projected loads. The model errors influencing these two conditions are strongly correlated since the model error for either condition is based on the product of numerous non-quantified factors that are presumed to be constant in the analysis. Another source of possible error in the analysis concerns the coefficients used in the

Table 2
Current (base period: 1981–2000) and projected changes in average-annual air temperature, total precipitation, total streamflow, total phosphorus load, and average volumetrically weighted phosphorus concentration (mg/L) by 2046–2065 for the entire Lake Michigan Basin based on eight General Circulation Models (GCMs) applied to three different greenhouse gas emission scenarios.

	Air temperature, °C			Precipitation, mm			Flow, m^3/s			Load (MT)			Volumetrically weighted concentration (mg/L)		
GCM	1981–2000	2046–2065	Difference	1981–2000	2046–2065	Percent difference	1981–2000	2046–2065	Percent difference	1981–2000	2046–2065	Percent difference	1981–2000	2046–2065	Percent difference
Average for each GCM and three greenhouse gas emission scenarios for 2046–2065															
CGM3	7.2	10.0	2.8	857	903	5.3	1388	1361	−1.9	4710	4630	−1.7	0.108	0.108	0.2
CNRM	7.2	9.7	2.5	871	919	5.6	1418	1383	−2.5	4832	4692	−2.9	0.108	0.108	−0.4
CSIRO	7.0	9.8	2.9	818	919	12.3	1352	1426	5.5	4634	4952	6.9	0.109	0.110	1.3
GFDL	7.0	9.5	2.5	820	810	−1.1	1305	1238	−5.1	4363	3991	−8.5	0.106	0.102	−3.6
GISS	6.8	9.0	2.2	835	921	10.2	1347	1425	5.7	4542	4859	7.0	0.107	0.108	1.2
MIUB	7.2	10.7	3.4	862	841	−2.4	1387	1172	−15.5	4770	3732	−21.8	0.109	0.101	−7.4
MPI	7.0	9.2	2.2	855	881	3.1	1413	1370	−3.0	4836	4645	−4.0	0.109	0.107	−1.0
MRI	7.1	9.2	2.1	823	891	8.3	1314	1353	3.0	4436	4468	0.7	0.107	0.105	−2.2
Average	**7.1**	**9.6**	**2.6**	**843**	**886**	**5.1**	**1365**	**1341**	**−1.8**	**4640**	**4496**	**−3.1**	**0.106**	**0.105**	**−1.4**
A1B greenhouse gas emission scenario															
CGM3	7.2	10.4	3.2	857	924	7.8	1388	1395	0.6	4710	4733	0.5	0.106	0.105	−0.1
CNRM	7.2	10.1	2.8	871	964	10.6	1418	1466	3.4	4832	5095	5.4	0.106	0.108	2.0
CSIRO	7.0	10.2	3.3	818	861	5.2	1352	1257	−7.0	4634	4132	−10.8	0.107	0.103	−4.1
GFDL	7.0	9.9	2.9	820	781	−4.7	1305	1153	−11.6	4363	3624	−16.9	0.105	0.099	−6.0
GISS	6.8	9.2	2.4	835	937	12.2	1347	1455	8.0	4542	4978	9.6	0.105	0.106	1.5
MIUB	7.2	10.8	3.6	862	877	1.8	1387	1244	−10.3	4770	4075	−14.6	0.107	0.103	−4.7
MPI	7.0	9.6	2.6	855	900	5.2	1413	1394	−1.3	4836	4735	−2.1	0.106	0.106	−0.7
MRI	7.1	9.5	2.4	823	920	11.9	1314	1415	7.7	4436	4727	6.6	0.105	0.104	−1.1
Average	**7.1**	**10.0**	**2.9**	**843**	**895**	**6.3**	**1365**	**1347**	**−1.3**	**4640**	**4512**	**−2.8**	**0.106**	**0.104**	**−1.7**
A2 greenhouse gas emission scenario															
CGM3	7.2	10.2	3.0	857	894	4.3	1388	1344	−3.1	4710	4530	−3.8	0.106	0.105	−0.7
CNRM	7.2	9.9	2.7	871	911	4.6	1418	1359	−4.2	4832	4547	−5.9	0.106	0.104	−1.8
CSIRO	7.0	10.0	3.1	818	941	15.0	1352	1483	9.7	4634	5291	14.2	0.107	0.110	4.1
GFDL	7.0	9.6	2.6	820	852	4.0	1305	1335	2.3	4363	4413	1.1	0.105	0.103	−1.1
GISS	6.8	9.3	2.6	835	933	11.7	1347	1468	8.9	4542	5057	11.3	0.105	0.107	2.2
MIUB	7.2	11.2	4.0	862	828	−3.9	1387	1093	−21.2	4770	3356	−29.6	0.107	0.097	−10.7
MPI	7.0	9.1	2.1	855	895	4.6	1413	1401	−0.9	4836	4761	−1.6	0.106	0.106	−0.7
MRI	7.1	9.4	2.3	823	863	5.0	1314	1252	−4.6	4436	4112	−7.3	0.105	0.103	−2.8
B1 greenhouse gas emission scenario															
CGM3	7.2	9.3	2.1	857	889	3.8	1388	1343	−3.2	4710	4627	−1.8	0.106	0.107	1.5
CNRM	7.2	9.2	2.0	871	883	1.4	1418	1322	−6.8	4832	4433	−8.3	0.106	0.105	−1.6
CSIRO	7.0	9.3	2.3	818	954	16.7	1352	1539	13.9	4634	5431	17.2	0.107	0.109	2.9
GFDL	7.0	9.0	2.0	820	798	−2.7	1305	1227	−5.9	4363	3937	−9.8	0.105	0.101	−4.1
GISS	6.8	8.4	1.7	835	892	6.8	1347	1352	0.3	4542	4542	0.0	0.105	0.105	−0.3
MIUB	7.2	10.0	2.7	862	818	−5.1	1387	1179	−15.0	4770	3765	−21.1	0.107	0.100	−7.1
MPI	7.0	8.8	1.9	855	850	−0.6	1413	1316	−6.8	4836	4438	−8.2	0.106	0.106	−1.5
MRI	7.1	8.8	1.7	823	889	8.0	1314	1392	5.9	4436	4566	2.9	0.105	0.102	−2.8

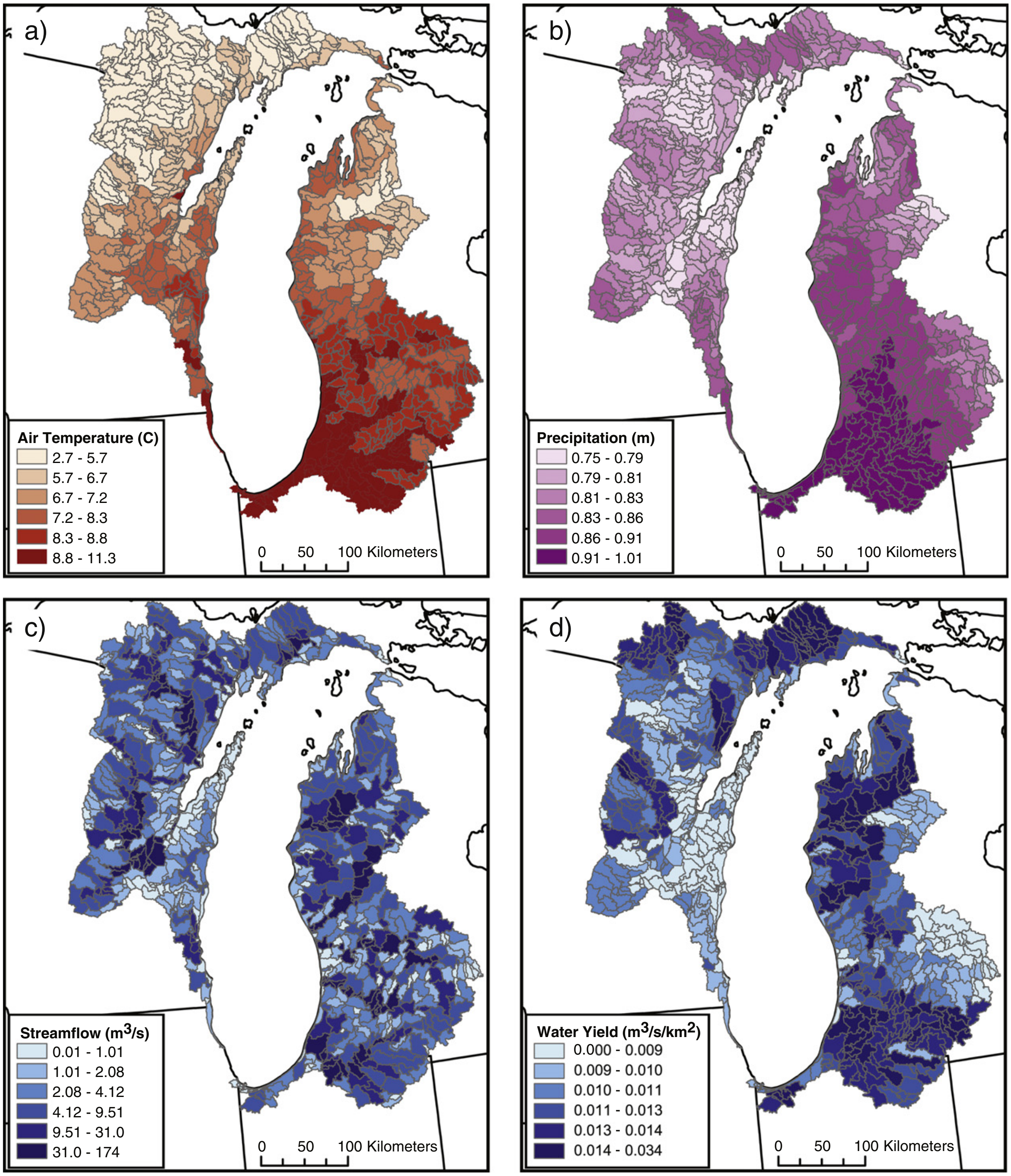

Fig. 2. Present (base period: 1981–2000) climate and hydrology: a) air temperature, b) precipitation (Notaro et al., 2011, 2014), c) streamflow, and d) water yield (Christiansen et al., 2014) for the Lake Michigan Basin.

original GCM, PRMS, and SPARROW models. These errors tend to approach zero as sample size gets large, but no attempt was made to evaluate the effects of these errors. To reduce the influence of model error in evaluating the climate induced changes in P loading to LM, most of the following results are described in terms of percent changes from the simulated 1981–2000 base conditions.

Projected future (2046–2065 and 2081–2100) conditions

All eight GCMs, for all three future greenhouse gas emission scenarios, project an increase in average-annual air temperatures throughout the LMB in the future. The average air temperature of the entire LMB was computed based on spatially weighting air temperatures over the entire land area (Fig. 4a). By 2046–2065, average-annual air temperature of the entire LMB is estimated to increase by 1.7 to 4.0 °C, depending on the GCM and emission scenario. Increases in air temperatures were smallest for the lowest greenhouse gas emission scenario (B1), and relatively similar for the most likely and high emission scenarios (A1B and A2). The average change in air temperature by the middle of the century, over the 24 different simulations, was an increase of 2.6 °C. Increases in air temperatures are not expected to be uniform throughout the LMB; each model and scenario has slightly different

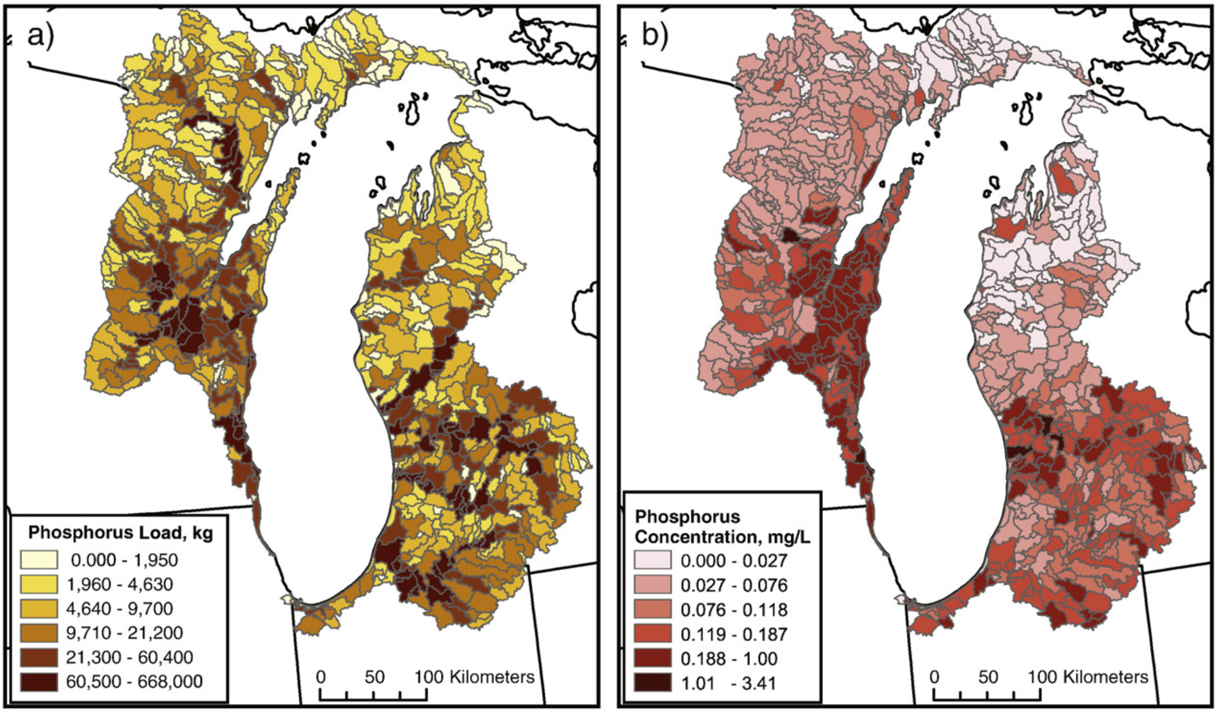

Fig. 3. Present (early 2000s) a) phosphorus loading and b) total phosphorus concentrations for the streams in Lake Michigan Basin based on results from the Upper Midwest SPARROW Model developed by Robertson and Saad (2011).

distributions in the increases in air temperatures. Distributions of the changes in air temperatures are shown for the average of all 24 scenarios in Fig. 5a. On average, largest changes in air temperatures are projected in the western and northern parts of the LMB. The changes observed for each simulation continued to increase from 2046–2065 to 2081–2100 (Fig. 4a). By 2081–2100, average-annual air temperatures are estimated to increase by 2.0–6.2 °C (average: +4.1 °C). Distributions of the changes for the largest P-load decrease scenario and the highest

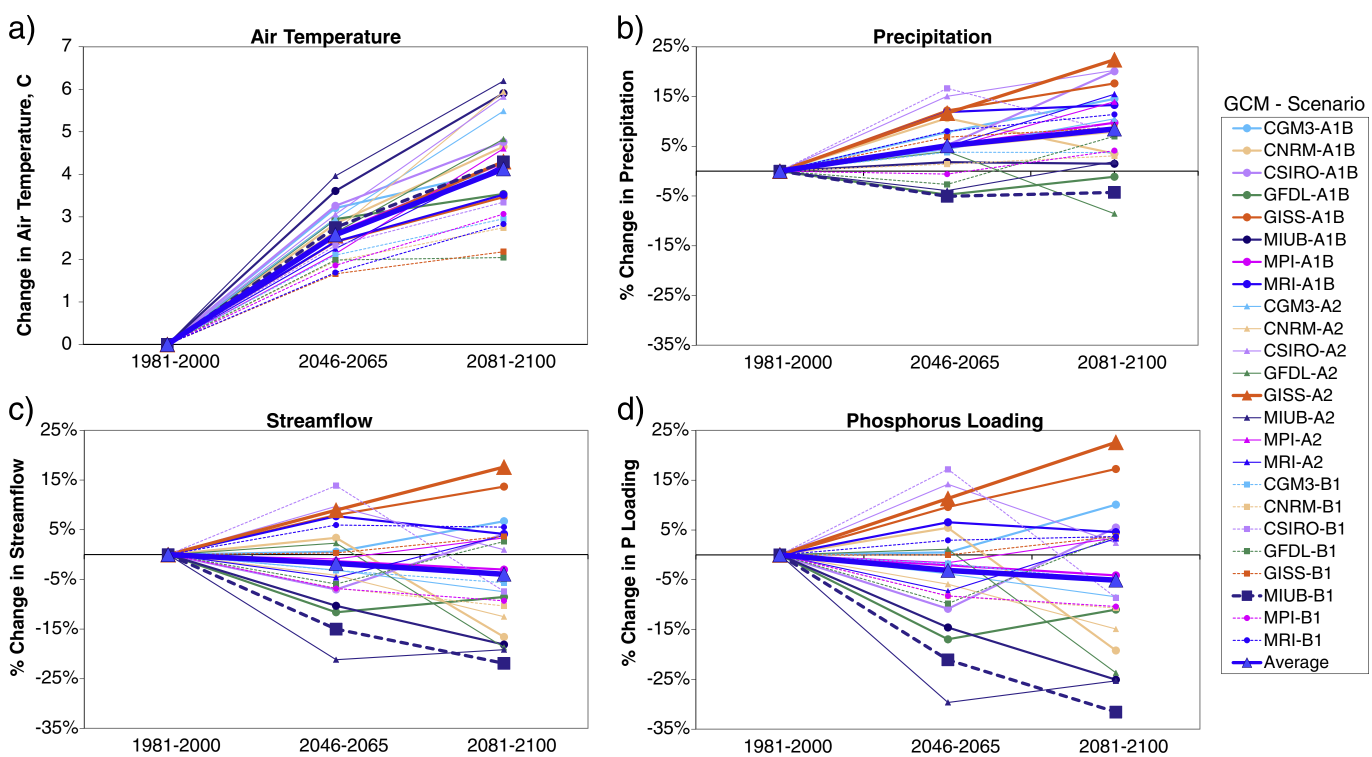

Fig. 4. Simulated a) average-annual air temperature, b) average total-annual precipitation, c) total average-annual streamflow, and d) total average-annual phosphorus loading for the present (base period: 1981–2000), mid-21st century (2046–2065), and late 21st century (2081–2100) for the entire Lake Michigan Basin based on eight different downscaled GCMs applied to three different future greenhouse gas emission scenarios.

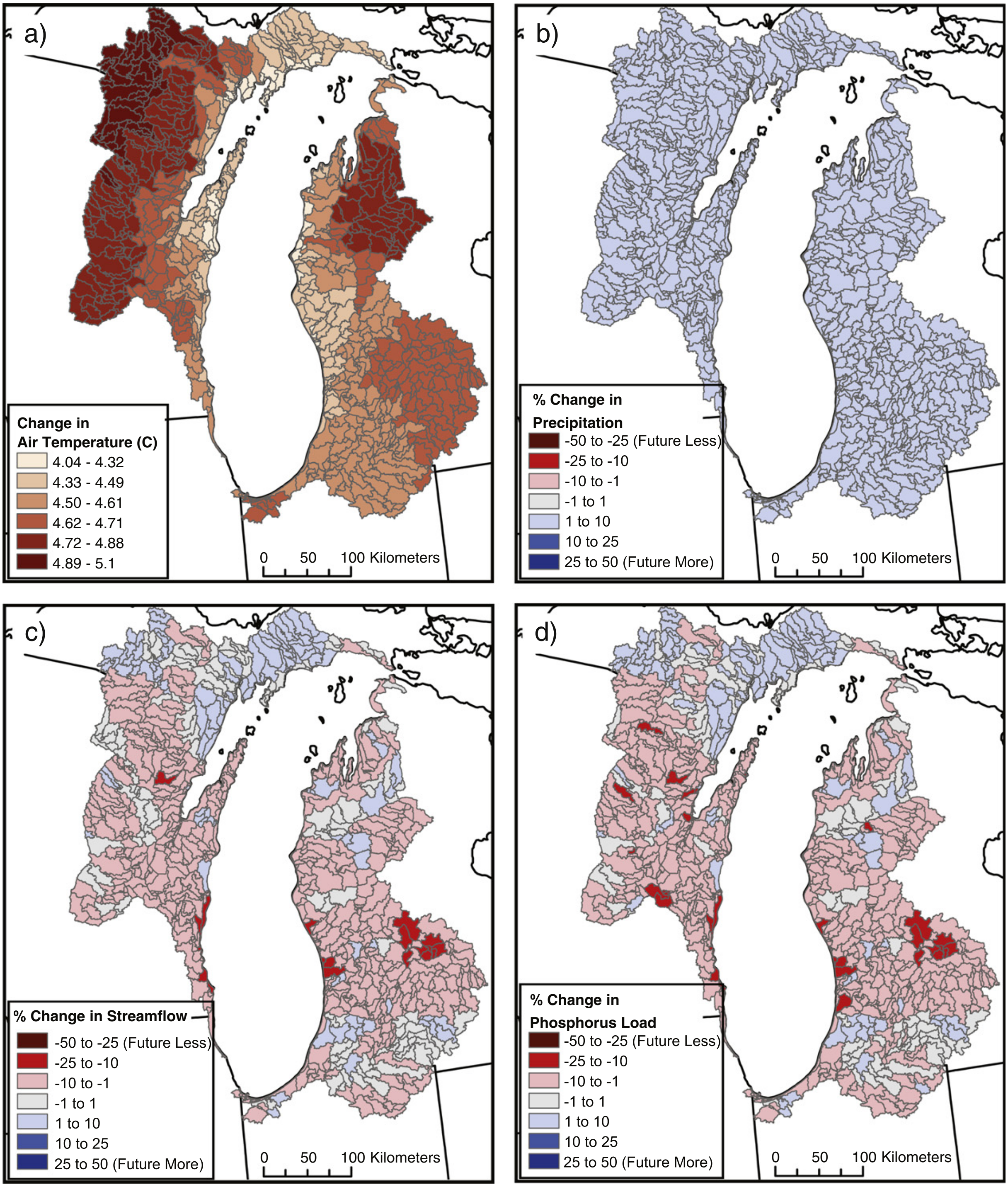

Fig. 5. Average projected changes from 1981–2000 to 2046–2065 in a) average-annual air temperature, b) average total-annual precipitation, c) total average-annual streamflow, and d) total average-annual phosphorus loading for catchments throughout the Lake Michigan Basin, based on eight GCMs, each applied to three different greenhouse gas emission scenarios.

P-load increase scenario are shown in the ESM Figs. S1 and S2 to demonstrate the extremes in the envelope for projected P loading.

All of these changes in air temperatures reflect changes in average-annual values; however, the GCMs, in general, project that the changes in air temperatures should be more dramatic in fall and early winter than the rest of the year (Notaro et al., 2011, 2014).

Projected changes in precipitation varied among GCMs and emission scenarios (Fig. 4b); however, the changes generally varied more by GCM than by emission scenario. In other words, most individual GCMs projected precipitation to either increase or decrease in the future regardless of the emission scenario. The average total-annual precipitation for the entire LMB was computed based on spatially weighting precipitation over the entire land area. By 2046–2065, average total-annual precipitation for the entire LMB is estimated to change ranging from a 5.1% decrease to a 16.7% increase (average: +5.1%) depending on GCM and emission scenario (Table 2). Distributions of the changes in precipitation are shown for the average of all 24 simulations in Fig. 5b. By 2081–2100, average total-annual precipitation over the entire LMB is estimated to change ranging from an 8.6% decrease to a 22.4% increase (average: +8.5%), depending on GCM and emission scenario.

Distributions of the changes for the largest P-load decrease scenario and highest P-load increase scenario are shown in ESM Figs. S1 and S2.

All of these changes in precipitation reflect changes in average total-annual values; however, in general, the GCMs predict that there will be more winter precipitation and less summer precipitation (Notaro et al., 2011, 2014). In addition, more of the winter precipitation should occur as rain rather than snow because of increased winter air temperatures.

Projected changes in streamflow varied among GCMs and emission scenarios (Fig. 4c). As with precipitation, changes in streamflow varied more by GCM than by emission scenario. By 2046–2065, the change in the total average-annual streamflow from the entire LMB is estimated to range from a 21.2% decrease to a 13.9% increase (average: −1.8%) depending on GCM and emission scenario. Distributions of the changes in streamflow are shown for the average of all 24 simulations in Fig. 5c. The average of all of the simulations demonstrates a small increase over the northern part of the LMB and a small decrease over the southern two-thirds of the LMB. Projected changes in streamflow were much more extreme for a few of the GCMs. Streamflows throughout almost the entire LMB are projected to decrease by the MIUB GCM, especially for the B1-scenario (ESM Fig. S1). In that scenario, streamflows for much of the LMB are projected to decrease by 10–25%. Streamflows throughout almost the entire LMB are projected to increase by the GISS GCM, especially for the A2-scenario (ESM Fig. S2). In that scenario, streamflows in the southern part of the LMB are projected to increase by 10–25%. By 2081–2100, total average-annual streamflow is estimated to change ranging from a 21.9% decrease to a 17.4% increase (average: −4.0%), depending on GCM and emission scenario (Fig. 4c). In general, the changes in streamflow for both periods had slightly larger ranges in change than the changes in precipitation, and were about 5–10% less than the changes in precipitation. In other words, the changes in streamflow had a wider envelope, but the envelope shifted downward compared to the envelope for the changes in precipitation in Fig. 4.

All of these changes in streamflow reflect changes in average-annual values; however, PRMS results indicate there should be less seasonality in flow. Because more winter precipitation will fall as rain, there should be more early winter runoff resulting in the magnitude of spring flows decreasing, and more recharge to groundwater resulting in higher baseflows (Christiansen et al., 2014).

Projected changes in P loading varied among GCMs and emission scenarios (Fig. 4d). Similar to precipitation and streamflow, changes in P loading varied more by GCM than by emission scenario. By 2046–2065, the change in the total average-annual P loading from the entire LMB is estimated to range from a 29.6% decrease to a 17.2% increase (average: −3.1%). Distributions of the changes in P loading are shown for the average of all 24 scenarios in Fig. 5d. The patterns in the changes in P loading are very similar to those for streamflow, with small increases over the northern part of the LMB and small decreases over the southern two-thirds of the LMB. Highest P loading rates are typically from the southern part of the LMB (Fig. 3), which resulted in the overall decrease in total P loading being larger than expected directly from the areal percent changes in Fig. 5. Predicted changes in P loading were more extreme for a few GCMs. P loading throughout almost the entire LMB was predicted to decrease by the MIUB GCM, especially for the B1-scenario (ESM Fig. S1). In that scenario, P loadings for much of the LMB are projected to decrease by 10–25%. P loadings throughout almost the entire LMB were predicted to increase by the GISS GCM, especially for the A2-scenario (ESM Fig. S2). In that scenario, P loadings in the southern part of the LMB are projected to increase by 10–25%. By 2081–2100, total average-annual P loading is estimated to change

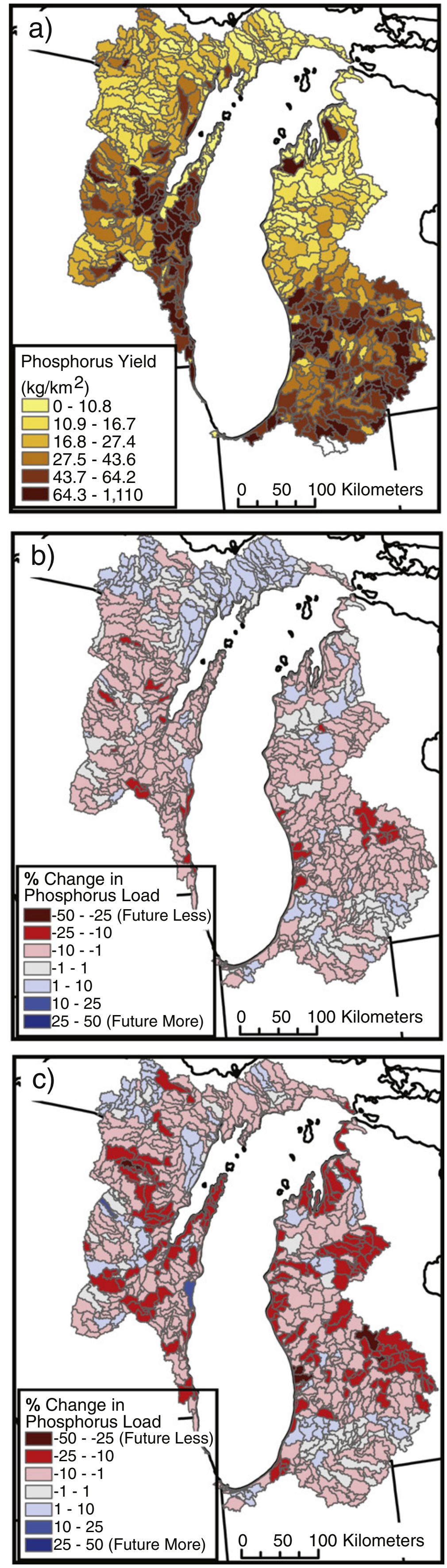

Fig. 6. Delivered phosphorus yield (delivered load per unit area) from catchments throughout the Lake Michigan Basin (LMB) for the a) present (base period: early 2000s), and average changes throughout the LMB from b) 1981–2000 to 2046–2065, and c) 1981–2000 to 2081–2100 based on eight GCMs, each applied to three different greenhouse gas emission scenarios.

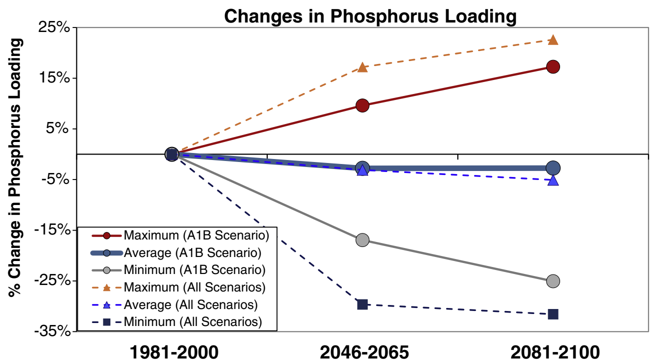

Fig. 7. Simulated total average-annual phosphorus loading for the present (base period: 1981–2000), mid-21st century (2046–2065), and late 21st century (2081–2100) for the entire Lake Michigan Basin based on eight different downscaled GCMs applied to the most likely (A1B) greenhouse gas emission scenarios.

ranging from a 31.6% decrease to a 22.6% increase (average: −5.1%), depending on GCM and emission scenario (Fig. 4d). The envelope for the changes in P loading was about 5–10% wider than the envelope for the changes in streamflow. In other words, increases in P loading were larger than the projected increases in streamflow and the decreases in P loading were more extreme than projected decreases in streamflow. This wider envelope is due to changes in P losses during downstream transport (discussed below).

Current and projected future changes in average-annual P yields throughout the LMB are shown in Fig. 6. Based on the average of the 24 scenarios, by 2046–2065, there could be a small increase in yields in the northern part of the LMB and decrease in yields in the southern two-thirds of the basin. Most decreases occur in areas with highest original P yields, which results in the overall decrease in loading being more than expected based only on the percent change in yield plots. Changes in yields become more dramatic by 2081–2100, with decreases occurring throughout almost the entire LMB. Many areas, projected to have small increases in P yields by 2046–2065, have decreases in yields later in the century, especially the north-central part of the LMB. Many areas with projected decreases in P yields in the central part of the basin have more extreme decreases by the end of the century (greater than 10%). Projections for the end of the century are more extreme than those demonstrated in Fig. 5 and are provided in the ESM Table S2.

In addition to examining changes in total P loading from all 24 scenarios (Fig. 4d), results from the most likely emission scenario (A1B) were examined separately (Fig. 7). Results from only the most likely emission scenario had a similar average change in P loading to LM (−2.8%) by 2046–2065, but slightly reduced the magnitude of the envelope, with projected changes ranging from a 16.9% decrease to 9.6% increase in loading. Because of the wide range in the differences in precipitation projected by the various GCMs (Fig. 4b) even when examining a specific emission scenario, there is still a wide range in projected changes in P loading to LM.

Discussion

Use of SPARROW to simulate future changes in climate

Rather than simply adjusting the land-to-water delivery variables in SPARROW to simulate the effects of climate change on P loading, PRMS was first used to simulate the changes in streamflow in response to changes in air temperature and precipitation. Then SPARROW was used to simulate how these changes in streamflow and velocity should affect in-stream P concentrations due to changes in-stream/in-reservoir losses. Finally HydroSPARROW was used to combine these results to project the changes in P loading. There are two reasons for using this approach rather than using SPARROW by itself: 1) the SPARROW model used in this study (Robertson and Saad, 2011) did not have climatic variables included as land-to-water delivery variables, which are often included in the model; and 2) land-to-water delivery variables in SPARROW, also referred to as spatial variability factors, should not be adjusted to evaluate such things as effects of climate change because the magnitude of the coefficient associated with each of these variables often depends on which other land-to-water delivery variables are included in the model (Schwarz et al., 2006). In other words, because the land-to-water delivery variables do not represent all of the factors operating in an actual ecosystem, interpreting the causative effect of any single land-to-water delivery variable is difficult (Robertson and Saad, 2013).

Climatic factors affecting streamflow and phosphorus loading

Based on the results from this study, projected changes in precipitation have more dramatic effects on future streamflow and P loading than the changes in air temperature. In general, average-annual streamflow and P loading increases as precipitation increases and decreases as precipitation decreases; however, warmer air temperatures increase evapotranspiration and results in an offset in this relation in terms of the percentage of change. The increases in air temperature by 2046–2065 alone should decrease streamflow by about 3–8%. Therefore, although on average (average of 24 scenarios) precipitation over the entire LMB is projected to increase by 5.1%, total average-annual streamflow is expected to decrease by 1.8% (PRMS results). However, because the projected changes in precipitation are generally larger than 3–8%, changes in streamflow are generally of the same sign as the changes in precipitation. Average-annual P loading is projected to follow the changes in streamflow; however, the changes in loading are expected to be more extreme because of changes in P losses during downstream transport. Based on the overall average and the average of the most likely eight scenarios, total P loading to LM should decrease by 3% by the middle of the 21st century.

Based on the overall average or the average for the most likely emission scenarios, P loading is only expected to change by 3% by mid-century: however, results from several scenarios are much different than the average. Therefore, unless there is a reason to believe the results of specific GCMs or specific emission scenarios more than others, in addition to looking at the overall average, it is important to develop and examine the plausible envelopes describing the range in all of the projections to build awareness of the potential changes that may occur in the future (USEPA, 2013). By the middle of this century (2046–2065), results of downscaled GCMs project that average-annual precipitation across the LMB may change −5% to +15%, causing total streamflow to change −18% to +12%, which in turn may cause annual-average P loading to change −29.6% to +17.2% (−16.9% to +9.6% for the most likely emission scenario). In addition to specific GCM simulations projecting larger changes than others, each scenario demonstrates that some areas of the LMB could have more dramatic changes than other areas. Largest changes are generally projected to occur in the southern part of the LMB. Therefore, future climatic changes could greatly affect the water quality of LM, especially in specific areas.

Changes in phosphorus concentrations caused by changes in downstream delivery

The changes in future P loading are slightly larger than the projected changes in streamflow because HydroSPARROW adjusts volumetrically weighted P concentrations based on how quickly water is delivered downstream. If streamflow increases, the model assumes that water is transported more quickly and there is less P lost during downstream transport. If streamflow decreases, water moves more slowly and there is more in-stream losses. The changes in travel time result in a plausible envelope for future volumetrically weighted P concentrations (Fig. 8). By the middle of this century (2046–2065), the average

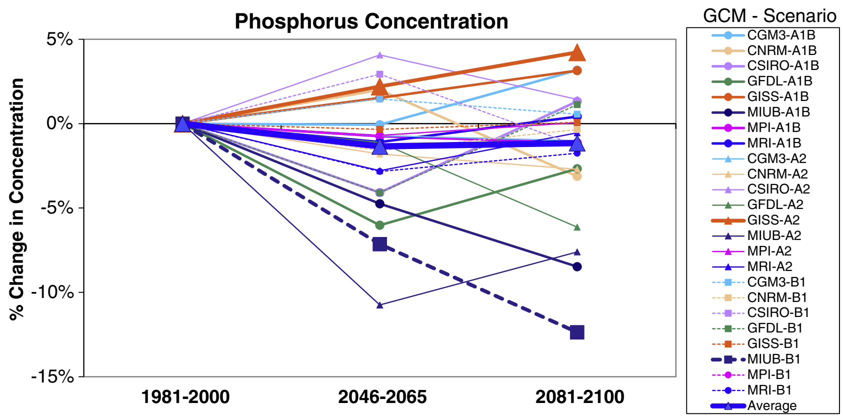

Fig. 8. Simulated volumetrically weighted total phosphorus concentrations for the present (base period: 1981–2000), mid-21st century (2046–2065), and late 21st century (2081–2100) for the entire Lake Michigan Basin based on eight different downscaled GCMs applied to three different future greenhouse gas emission scenarios.

concentration for the entire LMB is projected to decrease by 1.4%, but the full range is from −10.7% (for decreased flow with more in-stream losses) to +4.1% (for increased flow with less in-stream losses). Distributions of the changes in the average volumetrically weighted P concentrations projected for 2046–2065 are shown in ESM Fig. S3. By 2081–2100, P concentrations are projected to decrease by 1.2% on average, but range from −12.4% to +4.2%.

Comparison of the climatic response with those of other studies

A few other studies have examined how streamflow and P loading may change in response to future climate change, including two studies in the Great Lakes region. Most of these studies have projected that future P loading should increase primarily due to increased overall streamflows or increased short-term peak streamflows (Bosch et al., 2014; USEPA, 2013; Whitehead et al., 2009). However, because change in precipitation is the most important climatic factor affecting streamflow and because this factor varies dramatically among GCM and emission scenarios, it is important to examine the magnitude of the projected changes in precipitation being simulated. In a study by the USEPA (2013), 20 watersheds from throughout the U.S. were examined to assess the sensitivity of streamflow, and nutrient and sediment loads to changes in climate and urban development, including several watersheds draining into Lake Erie. In that study, they examined the response to several downscaled GCM projections: total average-annual precipitation changed from −8% to +14% for the Great Lakes watersheds, similar to that examined in this study (−5% to +15%). They projected that these changes would result in a change in average total-annual streamflow of −12% to +50%, which is higher than that projected in this study (−18% to +12%). The changes in streamflows in their study were primarily caused by their watershed model (SWAT) projecting lower (with less precipitation) and higher (with more precipitation) peak flows in the future. The USEPA study then projected that these flows would cause a change in P loads of −12% to +50%, or a change in P loads similar to the change in streamflow, compared to a range of −29.6% to +17.2% in this study. Therefore, their estimated volumetrically weighted P concentrations were projected not to change as streamflow changes.

Bosch et al. (2014) examined how streamflow, and nutrient and sediment loadings from four watersheds draining into Lake Erie should change in response to only two climate changes scenarios: moderate and more pronounced climate change scenarios, with only increases in total average-annual precipitation: +3% and +6%, respectively. The increases in precipitation resulted in changes in average-annual streamflow of +6% to +12%, and total average-annual P loading of +4% to +6%. Therefore, they projected changes in streamflow larger than the increases in precipitation, similar to that found by the USEPA (2013). The projected increases in P loading estimated by Bosch et al. (2014), however, were less than the projected changes in streamflow, which infers that their estimated volumetrically weighted P concentrations should decrease in the future as streamflow increases.

Changes in streamflow relative to changes in precipitation

The main difference in the results from our study and those of these other studies was caused by the differences in projected future precipitation. However, even after compensating for these differences, there are other factors that lead to differences in projected P loading, such as the relative changes in future streamflow (flow per unit precipitation, and changes in seasonality and intensity). Our study, which used projected long-term average-annual changes in streamflow based on daily projected flows from PRMS, found that streamflow generally increases with more precipitation and decreases with less precipitation; however, in the future, because of increased evapotranspiration caused by increased air temperatures, there should be less streamflow per unit precipitation. Whereas, studies by the USEPA (2013) and Bosch et al. (2014) both found that high-flow events may occur more often in the future, resulting in total average-annual streamflow increasing more than precipitation (on a percent basis).

To further investigate the response in streamflow to changes in precipitation with changes in air temperature, the ratio of average-annual streamflow to total annual precipitation as a function of average-annual air temperature were examined for two rivers in the LMB (Manitowoc and St. Joseph Rivers) and one in the Lake Erie Basin (Maumee River, where the other similar studies were conducted) for their period of available record (1930–1972 to present). Results for the Manitowoc River are shown in Fig. 9 (results for the other sites are

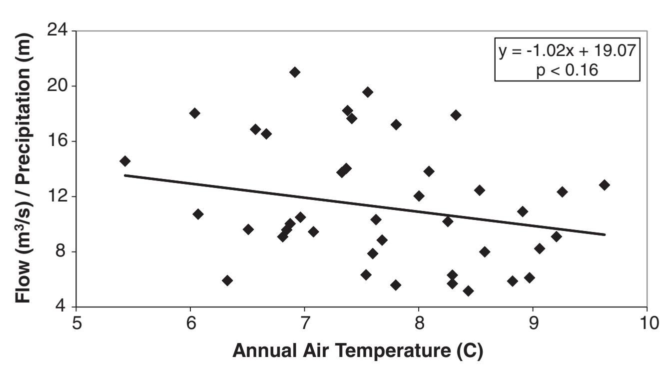

Fig. 9. Response in total average-annual streamflow per unit precipitation as a function of changes in average-annual air temperature (from Manitowoc, Wis.) for the Manitowoc River, station number 04085427, in the Lake Michigan Basin.

shown in ESM Fig. S4). Daily weather records for a downstream location on each river were obtained from NWS Cooperative Observers (http://mrcc.isws.illinois.edu/ accessed August 2015) and flow near the mouth of each river were obtained from U.S. Geological Survey (USGS) gaging stations (http://waterdata.usgs.gov/nwis/sw/ accessed August 2015). For each site, the ratio of average-annual streamflow to total annual precipitation decreased with increasing air temperature, although the relationships were not strong ($p < 0.12$–0.20). This indicates that average-annual streamflow may decrease as air temperatures increase, after compensating for differences in precipitation. This is consistent with that found in our study, and possibly caused by increased air temperatures causing more evapotranspiration leaving less water available for runoff.

Seasonality and intensity of streamflow may also change in the future. Christiansen et al. (2014) found that in the future there should be less seasonality in flow because more winter precipitation will fall as rain, which results in winter runoff being more spread out. This resulted in annual peaks in streamflow, which typically occur in spring, decreasing in the future. Other studies by the USEPA (2013) and Bosch et al. (2014), however, both concluded that high-flow events may occur more often in the future, and the USEPA (2013) study concluded that the annual peak flow may increase in the future. Winter and spring precipitation in the Great Lakes Region is expected to increase in the future by 20–30% (Bosch et al., 2014; Christiansen et al., 2014), but this may not affect the intensity of the highest runoff events that deliver the highest P loads because winter precipitation will fall more as rain and cause more runoff during the early winter months (Christiansen et al., 2014). Gebert et al. (2015) examined changes in streamflow in rivers throughout Wisconsin over the past 100 years. They found that peak annual streamflows, which typically occur in early spring, have decreased in recent years. Winter temperatures have increased in Wisconsin since the 1950s (WICCI, 2011). Therefore, although the number of moderate high-flow events may increase in the future (Mallakpour and Villarini, 2015; USEPA, 2013), peak annual flows which typically deliver the highest P loads may decrease in response warming air temperatures, consistent with that found in this study.

Changes in P concentrations relative to changes in streamflow

The HydroSPARROW approach results in changes in P loading having a larger range (wider envelope) than the changes in streamflow only because of changes in the volumetrically weighted P concentrations resulting from more in-stream losses with less (slower) flow and less in-stream losses during high (faster) flow (Fig. 8). Both of the previous studies suggested that the increase in P loading should be equal to (USEPA, 2013) or less than the increase in streamflow (Bosch et al., 2014), suggesting that average-annual volumetrically weighted P concentrations should either remain the same or decrease with increasing streamflow. Many studies have shown that P concentrations increase with increasing streamflow (for example see Robertson and Roerish, 1999; Richards and Baker, 1993). LaBeau et al. (2015) also showed that volumetrically weighted P concentrations increase with increasing flow for most streams in the GLB, unless they were dominated by point sources. However, LaBeau et al. showed that this relation should only slightly affect the overall annual volumetrically weighted P concentration because most of the increased flows occurred when P concentrations were relatively low (during winter and early spring). The increases in concentration with increasing flow and decreases in concentration with decreases flow used in this study are consistent with that found by LaBeau et al. (2015). Therefore, although the HydroSPARROW approach does not directly simulate the effects of short-term high-flow events, the short-term changes in streamflow are incorporated into the average-annual flows and the changes in average-annual volumetrically weighted P concentrations are consistent with those of other studies.

Relative importance of climate change and land-use change for P loading

Based on the overall average and the average for just the most likely emission scenario, total P loading to LM should decrease by about 3% by 2046–2065. However, other factors are expected to affect P loading besides climate change, especially changes in land use. Based on projected land-use changes in the absence of climate change, projected urban expansion in the LMB is estimated to increase P loadings by 4.9%, and additional agricultural expansion associated with predicted biofuel feedstock cultivation is estimated to further increase P loadings by 4.8%, for a total increase by 9.8% (LaBeau et al., 2014). The USEPA (2013) also projected that urban expansion by the middle of this century may increase P loading (P loadings from the Maumee River are projected to increase 1–5% depending on the GCM). Based on the average results of this study, the increases in P loading associated with land use change may be partly compensated for by decreases in P loading (3.1%) associated with decreases in streamflow resulting from the slight increases in precipitation being more than compensated for by increased evapotranspiration caused by increases in air temperatures. However, results of several of the climate-change scenarios suggest that P loading may increase in the future, which would further increase the loading anticipated from land-use change.

The land-use changes in the previous studies (LaBeau et al., 2015) were projected in the absence of climate change. In reality, there may be secondary effects of climate change, people will adapt to climate change resulting in additional shifts in land use, and with a longer growing season more fertilizers may be applied. In addition, warmer air temperatures may increase decomposition rates, which may affect the amount of nutrients transported downstream. Projecting these future land-use changes in response to climate change and incorporating these secondary affects into models like PRMS and HydroSPARROW is an area for future research.

Conclusions

Based on the average of eight downscaled GCMs, each applied to three greenhouse gas emission scenarios, P loading is not expected to dramatically change in the future; however, results from several GCMs project changes much different than the average. A few scenarios project P loading to increase by more than 10% by the middle of this century. Because of this variability in the projected changes in future climate, in addition to examining the overall average changes, it is important to develop and examine plausible envelopes in the potential changes, such as done in this study. These envelopes describe the range in the possible projections and provide information to build awareness of the potential changes that may occur in the future. The wide range in these envelopes is primarily caused by the various GCMs projecting different changes in precipitation and not caused by the different Greenhouse gas emission scenarios. Therefore, unless the IPCC and others determine that specific GCMs are more reliable than others, managers need to consider the full range of possible streamflows and P loadings to the Great Lakes and other water bodies to prepare for the future and determine what actions are needed to maintain P loading below the loading targets that are being set for the various systems. Only by maintaining P loadings below these targets can the potential eutrophication problems, such as that occurring in many nearshore areas, embayments, and even much of Lake Erie, be mitigated.

Acknowledgments

Partial funding for this project was provided by the U.S. Geological Survey National Water Quality Assessment Program. John Walker of the U.S. Geological Survey provided the PRMS hydrological data used in the analysis.

Appendix A. Supplementary data

Supplementary data to this article can be found online at http://dx.doi.org/10.1016/j.jglr.2016.03.009.

References

Alexander, R.B., Brakebill, J.W., Brew, R.E., Smith, R.A., 1999. ERF1—enhanced river reach file 1.2. U.S. Geol. Surv. Open-File Rep. 99–457.

Arnold, J.G., Kiniry, J.R., Srinivasan, R., Williams, J.R., Haney, E.B., Neitsch, S.L., 2012. Soil and Water Assessment Tool: Input and Output Documentation, Version 2012. Texas Water Resources Institute (TR–439, 654 pp.).

Bosch, N.S., Evans, M.A., Scavia, D., Allan, J.D., 2014. Interacting effects of climate change and agricultural BMPs on nutrient runoff. J. Great Lakes Res. 40, 581–589.

Brakebill, J.W., Terziotti, S.E., 2011. A digital hydrologic network supporting NAWQA MRB SPARROW modeling-MRB_E2RF1. http://water.usgs.gov/GIS/metadata/usgswrd/XML/mrb_e2rf1.xml.

Christiansen, D.E., Walker, J.F., Hunt, R.J., 2014. Basin-scale simulation of current and potential climate changed hydrologic conditions in the Lake Michigan Basin, United States. U.S. Geol. Surv. Sci. Invest. Rep. 2014–5175 (74 pp.).

DePinto, J.V. (U.S. co-chair), Lam, D. (Canadian co-chair), Auer, M., Burns, N., Chapra, S., Charlton, M., Dolan, D., Kreis, R., Howell, T., Rockwell, D., Scavia, D., 2006. Examination of the Status of the Goals of Annex 3 of the Great Lakes Water Quality Agreement. Report of the Annex 3 model review sub-group to the GLWQA Review Working Group D - Nutrients.

Dolan, D.M., Chapra, S.C., 2012. Great Lakes total phosphorus revisited: 1. Loading analysis and update (1994–2008). J. Great Lakes Res. 38, 730–740.

Gebert, W.A., Garn, H.S., Rose, W.J., 2015. Changes in streamflow characteristics in Wisconsin as related to precipitation and land use. U.S. Geol. Surv. Sci. Invest. Rep. 2015–5140.

IPCC (Intergovernmental Panel on Climate Change), 2007. Climate Change 2007: The Physical Science Basis. Contribution of Working Group I to the Fourth Assessment Report of the Intergovernmental Panel on Climate Change [Solomon, S., D. Qin, M. Manning, Z. Chen, M. Marquis, K.B. Averyt, M. Tignor and H.L. Miller (eds.)]. Cambridge University Press, Cambridge, United Kingdom and New York, NY, USA, (996 pp.)

LaBeau, M.B., Robertson, D.M., Mayer, A.S., Pijanowski, B.C., Saad, D.A., 2014. Effects of future urban and biofuel crop expansions on the riverine export of phosphorus to the Laurentian Great Lakes. Ecol. Model. 277, 27–37. http://dx.doi.org/10.1016/j.ecolmodel_2014.01.016.

LaBeau, M., Mayer, A., Griffis, V., Watkins, D., Robertson, D., Gyawali, R., 2015. Impact of discharge and climate on historical and future phosphorus exports from watersheds. Biogeochemistry 126, 153–172. http://dx.doi.org/10.1007/s100533-015-0149-5.

Mallakpour, I., Villarini, G., 2015. The changing nature of flooding across the central United States. Nat. Clim. Chang. 5, 250–254. http://dx.doi.org/10.1038/NCLIMATE2516.

Markstrom, S.L., Regan, R.S., Hay, L.E., Viger, R.J., Webb, R.M.T., Payn, R.A., LaFontaine, J.H., 2015. PRMS–IV, the precipitation-runoff modeling system, version 4. U.S. Geol. Surv. Techniques and Methods http://dx.doi.org/10.3133/tm6B7 (chap. B7, book 6, 158 pp.).

Michalak, A.M., Anderson, E., Beletsky, D., Boland, S., Bosch, N.S., Bridgeman, T.B., Chaffin, J.D., Cho, K.H., et al., 2013. Record-setting algal bloom in Lake Erie caused by agricultural and meteorological trends consistent with expected future conditions. Proc. Natl. Acad. Sci. 110, 6448–6452.

Moriasi, D.N., Arnold, J.G., Van Liew, M.W., Binger, R.L., Harmel, R.D., Veith, T.L., 2007. Model evaluation guidelines for systematic quantification of accuracy in watershed simulations. Trans. Am. Soc. Agric. Biol. Eng. 50 (3), 885–900.

Nakicenovic, N., Alcamo, J., Davis, G., de Vries, B., Fenhann, J., Gaffin, S., Gregory, K., Griibler, A., et al., 2000. Special Report on Emissions Scenarios: A Special Report of Working Group III of the Intergovernmental Panel on Climate Change. Cambridge University Press, Cambridge, U.K. (599 pp.).

Nechyba, T.J., Walsh, R.P., 2004. Urban sprawl. J. Econ. Perspect. 18, 177–200.

Notaro, M., Lorenz, D.J., Vimont, D., Vavrus, S., Kucharik, C., Franz, K., 2011. 21st century Wisconsin snow projections based on an operational snow model driven by statistically downscaled climate data. Int. J. Climatol. 31, 1615–1633.

Notaro, M., Lorenz, D., Hoving, C., Schummer, M., 2014. Twenty-first-century projections of snowfall and winter severity across Central-Eastern North America. J. Clim. 27, 6526–6550.

Pijanowski, B.C., Brown, D.G., Shellito, B.A., Manik, G.A., 2002. Using neural networks and GIS to forecast land use changes: a land transformation model. Comput. Environ. Urban. Syst. 26, 553–575.

Rathke, D.E., McRae, G., 1989. Great Lakes water quality board, report to the International Joint Commission. 1987 Report on Great Lakes Water Quality Great Lakes Surveillance vol. III ((1989) Appendix B).

Richards, R.P., Baker, D.B., 1993. Pesticide concentration patterns in agricultural drainage networks in the Lake Erie Basin. Environ. Toxicol. Chem. 12, 13–26.

Robertson, D.M., 1997. Regionalized loads of sediment and phosphorus to Lakes Michigan and superior — high flow and long-term average. J. Great Lakes Res. 23, 416–439.

Robertson, D.M., Roerish, E.D., 1999. Influence of various water-quality sampling strategies on load estimates for small streams. Water Resour. Res. 35 (12), 3747–3759. http://dx.doi.org/10.1029/1999WR900277.

Robertson, D.M., Saad, D.A., 2011. Nutrient inputs to the Laurentian Great Lakes by source and watershed estimated using SPARROW watershed models. J. Am. Water Resour. Assoc. 47 (5), 1011–1033. http://dx.doi.org/10.1111/j.1752-1688.2011.00574.x.

Robertson, D.M., Saad, D.A., 2013. SPARROW models to understand nutrient transport in the Mississippi/Atchafalaya River Basin. 42 (5), 1422–1440.

Schultze, S., 2005. Bradford is the dirtiest city beach. Milwaukee J. Sentinel (May 30, 2005).

Schwarz, G.E., Hoos, A.B., Alexander, R.B., Smith, R.A., 2006. The SPARROW surface water-quality model—theory, application, and user documentation. U.S. Geol. Surv. Techniques and Methods (book 6, chap. B3).

Sheffield, J., Barrett, A., Barrie, D., Carmargo, S.J., Chang, E.K.M., Colle, B., et al., 2014. Regional climate processes and projections for North America: CMIP3/CMIP5 differences, attribution and outstanding issues. NOAA Technical Report, OAR CPO-2, Climate Program Office, December 2014 (47 pp.).

Sun, L., Kunkel, L.E., Stevens, L.E., Buddenberg, A., Dobson, J.G., Easterling, D.R., 2015. Regional surface climate conditions in CMIP3 and CMIP5 for the United States: differences, similarities, and implications for the U.S. National Climate Assessment. NOAA Technical Report NESDIS 144 (111 pp.).

Taylor, K.E., Stouffer, R.J., Meehl, G.A., 2012. An overview of CMIP5 and the experiment design. Bull. Am. Meteorol. Soc. 93 (4), 485–498. http://dx.doi.org/10.1175/BAMS-D-11-00094.1.

USEPA (Environmental Protection Agency), 2013. Watershed Modeling to Assess the Sensitivity of Streamflow, Nutrient, and Sediment Loads to Potential Climate Change and Urban Development in 20 U.S. Watersheds. National Center for Environmental Assessment, Washington, DC (EPA/600/R-12/058F. Available from the National Technical Information Service, Alexandria, VA, and online at http://www.epa.gov/ncea).

USEPA (Environmental Protection Agency), 2015. Recommended phosphorus loading targets for Lake Erie. Annex 4 Objectives and Targets Task Team Final Report to the Nutrients Annex Subcommittee (http://www2.epa.gov/glwqa/report-recommended-phosphorus-loading-targets-lake-erie).

Vavrus, S.J., Notaro, M., Lorenz, D.J., 2015. Interpreting climate model projections of extreme weather events. Weather Clim. Extremes 10, 10–28.

Whitehead, P.G., Wilby, R.L., Battarbee, R.W., Kernan, M., Wade, A.J., 2009. A review of the potential impacts of climate change on surface water quality. Hydrol. Sci. J. 54 (1), 101–123. http://dx.doi.org/10.1623/hysj.54.1.101.

WICCI (Wisconsin's Changing Climate: Impacts and Adaptation), 2011n. Wisconsin Initiative on Climate Change Impacts. Nelson Institute for Environmental Studies. University of Wisconsin-Madison and the Wisconsin Dept. of Natural Resources, Madison, Wisc (217 pp.).

Zhou, Y., Obenour, D.R., Scavia, D., Johengen, T.H., Michalak, A.M., 2013. Spatial and temporal trends in Lake Erie hypoxia, 1987–2007. Environ. Sci. Technol. 47, 899–905.